Analysis of PSII antenna size heterogeneity of *Chlamydomonas reinhardtii* during state transitions

de Marchin Thomas[a], Ghysels Bart[a], Nicolay Samuel[b], and Franck Fabrice * [a]

[a]Laboratory of Bioenergetics, B22, University of Liège, B-4000 Liège/Sart-Tilman, Belgium
[b]Department of Mathematics, B37, University of Liège, B-4000 Liège/Sart-Tilman, Belgium

Accepted for publication in *Biochimica et Biophysica Acta (BBA) - Bioenergetics*, July 18, 2013
The original publication is available at http://www.sciencedirect.com/science/article/pii/S0005272813001266

Abstract

PSII antenna size heterogeneity has been intensively studied in the past. Based on DCMU fluorescence rise kinetics, multiple types of photosystems with different properties were described. However, due to the complexity of fluorescence signal analysis, multiple questions remain unanswered. The number of different types of PSII is still debated as well as their degree of connectivity. In *Chlamydomonas reinhardtii* we found that PSIIα possesses a high degree of connectivity and an antenna 2-3 times larger than PSIIβ, as described previously. We also found some connectivity for PSIIβ in contrast with the majority of previous studies. This is in agreement with biochemical studies which describe PSII mega-, super- and core- complexes in *Chlamydomonas*. In these studies, the smallest unit of PSII *in vivo* would be a dimer of two core complexes hence allowing connectivity. We discuss the possible relationships between PSIIα and PSIIβ and the PSII mega-, super- and core- complexes. We also showed that strain and medium dependent variations in the half-time of the fluorescence rise can be explained by variations in the proportions of PSIIα and PSIIβ. When analyzing the state transition process in vivo, we found that this process induces an inter-conversion of PSIIα and PSIIβ. During a transition from state 2 to state 1, DCMU fluorescence rise kinetics are satisfactorily fitted by considering two PSII populations with constant kinetic parameters. We discuss our findings about PSII heterogeneity during state transitions in relation with recent results on the remodeling of the pigment-protein PSII architecture during this process.

*Corresponding author : F.Franck@ulg.ac.be

1 Introduction

Photosynthesis is the process by which light energy is converted into chemical energy (ATP and NAD(P)H) usable for the synthesis of organic compounds. The first step of this process is the absorption of light by antenna pigments of PSI and PSII. Excitation energy is then transferred to reaction centers of the photosystems where photochemistry drives a flow of electrons and protons across the thylakoïd membrane, which permits the synthesis of ATP and NAD(P)H. The antenna of PSI is enriched in chlorophyll a and absorbs to longer wavelength than PSII which is enriched in chlorophyll b. Due to this, photosystems can be excited differently depending of the excitation light quality and this can lead to an imbalance of the electron transport chain. In order to correct this imbalance, LHCII antenna complexes can migrate between PSI and PSII and make their cross section to vary, thus restoring the excitation balance. This phenomenon, termed 'state transitions' has been discovered independently by Bonaventura and Myers and by Murata [1, 2].

State transitions have been extensively studied in *Chlamydomonas reinhardtii* because in this organism, up to 80% of the LHCII can migrate between the photosystems [3], against about 20-25% for higher plants. In *Chlamydomonas*, like in other studied organisms, the redox state of the plastoquinone (PQ) pool is the main determinant of state transitions through binding of plastoquinol to the Q_0 site of Cyt b_6f [4, 5]. Under conditions of over reduction of the PQ pool (due to over-excitation of PSII or to non-photochemical reduction by the NAD(P)H dehydrogenase NDA2), the kinase STT7 phosphorylates LHCII which then migrates to PSI (state II) [6]. Under conditions where the PQ pool is oxidized, STT7 kinase is inactivated and a constitu-

tively active phosphatase dephosphorylates LHCII antenna which then migrates to PSII (state I) [7, 8]. Rintamäki et al. showed that STT7 activation is not only under control of the PQ pool redox state but is also part of a complex network involving the thioredoxin/ferredoxin system [9].

In addition (and in relation) to their function in regulating the distribution of antenna pigment-proteins between PSI and PSII, state transitions can also control the relative electron fluxes through linear and cyclic electron transports [10, 11]. For cyclic electron transport to occur, it is admitted that ferredoxin reduced by PSI can reduce the PQ pool via the cyt b_6f, via an unknown ferredoxin:PQ oxidoreductase or via NAD(P)H thanks to NDA2 [12, 13, 14]. Cyclic electron transport is favoured over linear electron transport in state II, which permits the synthesis of extra ATP by the generation of a trans-thylakoidal electrochemical gradient in the absence of net production of reducing equivalents. Thus, regulation of cyclic electron transport by state transitions allows the cell to regulate the ratio of ATP to NADPH produced during the light-phase of photosynthesis.

It is well known that PSI and PSII are not homogeneously dispersed in the thylakoïd membrane. PSII is located mainly in the grana (appressed membrane region) but a small part is present in the stroma exposed (non-appressed) membrane region while PSI is strictly present in the latter [15, 16]. In addition to these heterogeneities, structural and functional heterogeneity has also been shown for different PSII sub-populations. PSII heterogeneity was first described by Melis and Homann based on previous observations that the fluorescence rise of dark-adapted chloroplast did not follow a first order reaction kinetics [17, 18]. Melis and Homann concluded to the existence of two PSII populations, namely the PSIIα and the PSIIβ [19, 20]. This was inferred from the analysis of the semilogarithmic plot of the kinetics of the complementary area (CA) above the fluorescence rise curve in presence of the inhibitor DCMU. This inhibitor binds the pocket Q_B of PSII and permits the photochemical reduction of the primary quinone Q_A without influence of its reoxidation by plastoquinones. Previous works showed [21, 22, 23] that the complementary area over the fluorescence rise curve (area between the fluorescence curve and a horizontal line at the maximal fluorescence level F_M) in presence of DCMU is proportional to the number of photosystems able to realize reduction of Q_A. Melis and Homann [19] found two phases in the time-dependent increase of the CA and ascribed them to the two populations of PSII. Since then, many studies have been conducted on this subject and a third phase has been discovered: phase γ [24, 25].

Phase α is ascribed to a sub-population of dimeric PSII localized in the appressed membrane region of the thylakoid [26]. They are characterized by an antenna of 210-250 chlorophylls [26] and connectivity (p). This term was proposed by Joliot and Joliot and is related to the transfer of absorbed energy from a closed reaction center (in which Q_A is already reduced) to an open neighboring unit [17]. Connectivity is reflected by a sigmoidal fluorescence rise. Phase β is ascribed to a population of monomeric PSII localized in the non-appressed membrane region of the thylakoid. They are characterized by an antenna 2 to 3 times smaller than PSIIα ($\backsim$130 Chl) and do not possess connectivity, which is reflected as an exponential fluorescence rise. The last γ phase is characterized by a rate 10 to 40 times slower than phase α but it seems that, in contrast to the two previous phases, it is not directly related to photoreduction of Q_A. Indeed, the rate constant of this γ phase behaves in a non-linear way towards light intensity [27]. The existence of four phases has been suggested [28] but most studies report only three phases (see [29] for review).

It is most often considered that the increase in fluorescence intensity during the DCMU-FR is essentially due to Q_A reduction, following the original theory of Duysens and Sweers [30], but other theories with different explanations for the slow phases of the DCMU-FR have emerged (reviewed in in [31]) such as fluorescence yield variations due to conformational changes [32, 33, 34]. Even if the different phases in the DCMU-FR are interpreted as reflecting different Q_A reduction kinetics, antenna size heterogeneity is not the only possible interpretation for these phases (other interpretations are reviewed in [29]). Differences in trapping efficiency could also result in the appearance of several phases. For example, a lower photochemical quantum yield for PSIIβ versus PSIIα would lead to an overestimation of the proportion of PSIIβ with the analysis of the semilogarithmic plot of the kinetics of the CA above the fluorescence rise curve. The comparison of the PSIIβ and PSIIα quantum yields has been conducted in the past. Although lower quantum yield for PSII associated to the slow phase of the induction kinetics (usually ascribed to phase β) has been reported [35, 18, 36, 37], other studies showed similar quantum yields for both types of PSII [38, 39]. It is clear that the case is not settled. In any case, even if a proportion of PSII had a lower quantum efficiency, the amplitude of this difference is too low to account entirely for the proportion of PSIIβ [29]. It was also suggested that the β phase was related to PSII being less sensitive to DCMU

addition [40], but this could be circumvented by using a sufficiently high DCMU concentration (20 μM) [41]. In any case, Melis and Duysens showed a very good correlation between the different phases in the absorbance changes at 320nm (reflecting Q_A reduction) and the different phases in DCMU-FR [35]. Moreover, biochemical studies demonstrated the existence of multiple PSII complexes with different antenna sizes (see below) and it must necessarily be reflected in a multi-phasic character of the DCMU-FR.

It should also be mentioned that other type of PSII heterogeneities (not related to the sole photoreduction of Q_A in presence of DCMU) have been described such as PSII reducing side heterogeneity, which refers to the ability of a reaction center to transfer electron to the secondary acceptor Q_B [29]. These will not be addressed here.

The proportions of PSIIα and PSIIβ are not fixed and vary with culture conditions as well as with sample preparation. It has been reported that protein phosphorylation of chloroplast membrane, that simulates state transition, leads to an increase in the amplitude of phase β whether by conversion of PSIIα into PSIIβ [42] or by preferential quenching of PSIIα [43, 44]. However, these studies, like most studies on PSII heterogeneity (with exception of the work of Lazár et al. and Nedbal, Trtílek, and Kaftan, [27, 45]) were conducted on chloroplast preparations or isolated thylakoids. The method of isolation of these organelles and their resuspension in various media are likely to influence the properties of the photosynthetic apparatus and the relevance of the results to the *in vivo* situation can be questioned. Other factors influencing the proportion of PSIIα and PSIIβ have been described such as temperature [46, 47], concentration in Mg^{2+} [44] , pH [20] and greening time in the case of higher plants [48, 49].

In addition to this description of heterogeneity by functional analysis of the fluorescence rise of PSII *in vivo*, biochemical studies have been conducted more recently. Methods used were mainly based on isolation of PSII complexes and subsequent analysis. Most studies report the existence of PSII megacomplexes composed of a dimer of supercomplex C_2S_2 where C refer to the PSII core complex and S to the *strongly* bound LHCII trimer (one LHC trimer and two LHC monomer). Other complexes have been reported in spinach chloroplast such as the $C_2S_2M_2$ supercomplex where two *moderately* bound LCHII trimers and one monomer bind the C_2S_2 supercomplex [50]. A third type of L (for *loosely* bound) LHC trimer may bind the supercomplex but the resulting complex would be rare [51]. In *Chlamydomonas reinhardtii*, the largest supercomplex detected is C_2S_2, probably due to the lack of CP24 [52], which is needed to bind M trimers.

A stepwise mechanistic model has been proposed for LHCII dissociation from PSII and reassociation with PSI after phosphorylation by the STT7 kinase during state transitions in *Chlamydomonas* [53, 54]. Initially, cells are in state 1 and unphosphorylated LHCII stabilize the PSII–LHCII megacomplex. First, the phosphorylation of LHCII type I in the major LHCII trimers triggers the dissociation of the megacomplex, resulting in individual C_2S_2 supercomplexes. Secondly, the increase in the phosphorylation of CP26 and CP29, as well as the PSII core subunits D2 and CP43 (although the role of the latter remains unclear), induces the displacement of remaining LHCII from the PSII core complex, resulting in discrete C_2 core complex. Finally, a part of dissociated phospho-LHCII migrates from the PSII-rich appressed region membrane to the PSI-rich non-appressed region membrane and associates with PSI [55, 56, 57, 58], leading to state 2 while the other part may aggregate to form an energy-dissipative complex [59, 60]. Nevertheless, the existence of a LHCII energy dissipative complex is in contradiction with results of Delosme, Olive, and Wollman who showed a complementary change in LHCII association with PSI and PSII upon state transition [3]. Recent results in *Arabidopsis thaliana* suggest that in addition to the control of LHC phosphorylation by STN7 kinase, the association/dissociation of supercomplexes is under the control of a new parallel but independent regulatory pathway involving Psb27 and PsbW proteins [61, 62].

The structural PSII heterogeneity, and the complexity of the rearrangement of pigment-protein complexes during state transitions, outlined above, are likely to have their counterpart in terms of changes in functional antenna size during state transitions. However, an in situ analysis of functional PSII heterogeneity from the fluorescence rise curve in presence of DCMU has not been performed. Here, we analyze PSII heterogeneity related to DCMU-FR in *Chlamydomonas reinhardtii* cells, we show how this heterogeneity is affected during state transitions and discuss the results in terms of changes in antenna size heterogeneity.

2 Material and methods

2.1 Strains and Growth Conditions

The *Chlamydomonas reinhardtii* wild-type strain *1690* used in this work was obtained from the *Chlamydomonas Resource Center*. The mutant *stt7*

unable to realize state transitions was obtained from J.-D. Rochaix [63]. Cells were grown at 25° C in Tris-acetate-phosphate medium [64] under 80 μmol PAR $m^{-2}s^{-1}$ continuous white light and regularly diluted to ensure that cells were in exponential phase. In section 3.2, other wild-type strain were used, such as strain *25* (derived from the CC-400 cw15 [65]) and strain *2'* (derived from the *wt* strain 137c [66]). In that section, cells were grown in Tris-acetate-phosphate medium and in Tris-buffered mineral media.

2.2 Chlorophyll concentration determination

Pigments were extracted from whole cells in ethanol and debris were removed by centrifugation at 10,000g for 5 min. The Chl (a + b) concentration was determined according to [67] with a lambda 20 UV/Vis spectrophotometer (Perkin Elmer, Norwalk, CT).

2.3 Chlorophyll fluorescence measurement

Chlorophyll fluorescence emission measurements were made using a PAM (pulse amplitude modulated) chlorophyll fluorimeter (type FMS 1, Hansatech instruments, UK). Prior to each measurement, cultures were dark-adapted for 30 minutes. The analytical light was provided by light-emitting diodes with an emission maximum at 594 nm. The frequency of measuring flashes was 1500 per second and their integral light intensity was less than 0.1 μmol PAR $m^{-2}s^{-1}$. F_M level was obtained by applying a pulse of saturating light (6000 μmol PAR $m^{-2}s^{-1}$) provided by a halogen light source. Measurements of chlorophyll fluorescence rise curve in presence of 20μM DCMU were made in cell suspensions (2 ml) using a AquaPen AP-C 100 fluorimeter (PSI, Czech Republic). The maximal intensity (100%) was 1670 μmol PAR $m^{-2}s^{-1}$ at 455 nm. Chlorophyll concentration was adjusted to 10 μg ml^{-1} for PAM measurements and to 1 μg ml^{-1} for chlorophyll fluorescence rise curve measurements.

2.4 Low temperature fluorescence spectra

Fluorescence emission spectra at 77K were recorded using a LS 50B spectrofluorimeter (Perkin Elmer). The excitation wavelength was 440 nm. Excitation and emission spectral width slits were 10 and 5 nm, respectively. A broad blue filter (CS-4-96, Corning, Corning, NY) was placed between the excitation window and the sample to minimize stray light. Cells were frozen in liquid nitrogen. Chlorophyll concentration was lower than 2 μg ml^{-1}, and it was verified that no changes in the intensity ratio of the 685 and 715 nm emission bands arose from reabsorption artefacts. Spectra were normalized to a fluorescence intensity of 1 at 685 nm.

2.5 Curve fitting

Fitting of the fluorescence rise in presence of DCMU was realized with the R package *nls* and the *port* algorithm. R is an open-source statistical software freely available under GNU license [68]. *Nls* package allows the simultaneous direct fitting of several curves of the DCMU-FR, which permits an increase in the reliability and accuracy in the determination of the model parameters [27]. It also gives the possibility to control which parameter is allowed to vary between curves and which cannot, depending of the experimental design (see [69] for a good manual on *nls*). The principle of non-linear regression is to minimize the square of the distance between experimental data and a theoretical curve (χ^2) by testing multiple combinations of parameters. The parameters giving the minimal χ^2 are then choosen for subsequent analysis. Comparison of the quality of fit by different models was realized using the R function *AIC*. When specified, the error range was determined using the R function *confint.nls*. This function calculates the χ^2 subsequent to a stepwise change of each parameter and determines if the new χ^2 is significantly worse than the χ^2 determined by the best fitting. This gives a confidence interval. The confidence level was set to 90%. For more information on error range determination, see [70, 39].

3 Results and discussion

Different approaches have been proposed for the determination of PSII antenna heterogeneity from the fluorescence rise in presence of DCMU (DCMU-FR). The original procedure of Melis and Homann is based on deconvoluting the time-course of the complementary area (CA) over the fluorescence rise curve. This approach suffers from two main problems. First, it requires a very accurate determination of the maximum level of fluorescence FM. This can be difficult since small distortions of the signal not attributable to photochemistry occur, such as caused by non-photochemical quenching (NPQ) and technical limitations of experimental apparatus. Bell and Hipkins showed that an error of 2% in F_M determination leads to an error of 150% in the amplitudes and rates of different photosystems [71].

Secondly, the determination of the contributions of the different phases starts by calculating the rate and amplitude of the slowest phase and subtracting it from the kinetics of the whole complementary area. This operation is repeated from the slowest phase to the last fastest phase. This implies that any small error in the determination of the first slow phase (the most inaccurate) affects the calculation of the next phases. Moreover, as discussed before, the slowest phase (γ) is not related to the photoreduction of Q_A and for this reason, determination of its kinetics and extent by the time course of the CA is not relevant.

In 1995, Trissl and Lavergne [72, 73] introduced a new method of determination of PSII heterogeneity based on direct fitting of the time course of the fluorescence rise. This method is more accurate than the Melis and Homann's original approach because mistakes due to an erroneous determination of F_M are avoided. Lazár et al. used this approach to determine PSII antenna heterogeneity of PSII on wheat leaves and *Chlamydomonas reinhardtii* cells [27]. The novelty of their study was in the simultaneous direct fitting of several curves of the DCMU-FR at different light intensities. This increases the reliability and accuracy of the determination of the model parameters.

In the presence of DCMU, the fluorescence rise (DCMU-FR) can be fitted with the equation :

$$rF_V(t) = \sum_{i=1}^{3} F\mathrm{PSII}_i \frac{(1-p_i)\mathrm{PSII}_i^{closed}(t)}{1-p_i\mathrm{PSII}_i^{closed}(t)} \qquad (1)$$

where $rF_V(t)$ is the normalized rise of fluorescence intensity, $F\mathrm{PSII}_i$ is the proportion of variable fluorescence associated to PSII of type i, p_i is the connectivity parameter described by Joliot and Joliot [17],t is the time and $PSII_i^{closed}(t)$ is the proportion of closed PSII of type i at time t. This last term is described by the equation

$$\mathrm{PSII}_i^{closed}(t) = \mathrm{PSII}_{i,0}^{open}(1-e^{(-k_i t)}) \qquad (2)$$

where $\mathrm{PSII}_{i,0}^{open}$ is the proportion of open PSII of type i at time 0 (which is 1 in case of dark adapted material) and k_i is the rate constant of reduction of the PSII. These equations, derived from Lazár et al. [27], allows a good fit of the DCMU-FR.

In theory, k_i is not a constant but varies with time due to excitation energy transfer between closed and open PSII. As the time increases, the increase in the proportion of closed PSII leads to an increase in the effective antenna size of open PSII. Thus, k_i(t) vary according to :

$$\mathrm{k}_i(t) = \frac{\mathrm{k}_i^0}{1-p_i\mathrm{PSII}_i^{closed}(t)} \qquad (3)$$

where k_i^0 is the initial rate constant when all PSII are open. However, there is no explicit solution to these 3 equations (see supplemental data), thus preventing the use of non-linear regression algorithm. To circumvent this problem, we could use an iterative process to fit our data (as used in [27]). The problem with such process is that it is difficult to know if the algorithm has converged to a suitable solution. In order to be able to use a regression algorithm, we considered k_i as a constant, characterizing the kinetics of a whole phase (thus, in our case, such a value k_i cannot be interpreted as a quantification of the initial rate constant k_i^0).

It is important to note that the proportion of fluorescence $F\mathrm{PSII}_i$ associated to each photosystem type represents the proportion of chlorophylls associated with each type of photosystem and is not a quantification of the proportion of each type of photosystem, due to their differences in antenna size. The proportion of photosystems $\omega\mathrm{PSII}_i$ can only be calculated from their contributions to the complementary area over the fluorescence rise curve (CA) [21, 23]. The proportion CA_i of the CA that corresponds to PSII_i has been calculated from the fluorescence rise associated to each PSII type. This is mathematically calculated after the regression procedure giving the p_i, k_i and $F\mathrm{PSII}_i$ parameters.

Most earlier fluorescence studies report the existence of three PSII types: PSIIα, PSIIβ and PSIIγ in which only PSIIα are able to share excitation energy (connectivity) between individuals units [29]. Is is tempting to ascribe the PSII mega-,super- and core- complexes described in most recent biochemical studies to the PSIIα, PSIIβ and PSIIγ. However, in earlier functional studies, the ability to share excitation energy between individuals units was restricted only to PSIIα while new biochemical evidences suggest a dimeric organization, and therefore the possibility for energy transfer between neighbouring units for all PSII complexes. There is, therefore, a need of comparing the suitability of models, which consider a connectivity term (p) either for PSIIα only, for PSIIα and PSIIβ or for all PSII types.

In order to decide which model is best adapted, we fitted DCMU-FR curves measured at different light intensities (same data as section 3.1) with the three models. In model 1, connectivity was allowed only for PSIIα. In model 2, it was allowed for PSIIα and PSIIβ whereas in model 3, it was allowed for all type of PSII. Usually, the quality of a fit is determined on the value of the χ^2. The lower it is,

the higher is the efficiency of the fit to describe the experimental data. However, comparing quality of models with different number of variables (in our case, more parameters due to connectivity for PSIIβ and PSIIγ) with the χ^2 is not appropriate because adding variables increases the complexity of the model and the number of solutions possible for the fit. It will always be possible to add artificial, non-biologically meaning parameters and increase the quality of the fit. Thus, to avoid overfitting, it is necessary to take into account the complexity of the model in the assessment of the quality of the fit. The *Akaike's information criterion* (AIC) permits the comparison of different models with different number of variables by judging the quality of the fit and introducing a penalty for the number of parameters used [74]. AIC was determined according to equation 4 where k is the number of parameters and L is the maximized value of the likelihood function for the estimated model. For more information on AIC, see Burnham and Anderson [75].

$$\mathrm{AIC} = 2k - 2\ln(L) \tag{4}$$

AIC for the three models is shown in table 1. The AIC of model 2 is lower than that of model 1 and model 3, which is an indication that model 2 describes the experimental data better than other models. Moreover, the difference between the two best models AIC_{model3} - AIC_{model2} is 18. Considering the rule of thumb given in Burnham and Anderson, which requires a difference in AIC of more than 10 to definitely choose one model over another model [75], we decided to make the subsequent fitting of DCMU-FR curve with model 2. Residuals of the fit for the three models are shown in figure S1. In contrast to what was described in most previous studies, we had to conclude that PSIIβ are characterized by a non 0 connectivity (only two former studies [72, 27] came to the same conclusion).

model	AIC	Δ_i
1: connectivity allowed only for PSIIα	-14599	2416
2: connectivity allowed for PSIIα and PSIIβ	-17025	0
3: connectivity allowed for PSIIα, PSIIβ and PSIIγ	-17007	18

Table 1: Determination of the best model to analyse PSII antenna size heterogeneity by calculating the AIC on the entire data set of section 3.1. In model 1, connectivity was allowed only for PSIIα. In model 2, it was allowed for PSIIα and PSIIβ whereas in model 3, it was allowed for all type of PSII. Δ_i represents the AIC differences : $\Delta_i = \mathrm{AIC}_i$ - AIC_{min}. Model 2 has been selected because it had the lower AIC value.

3.1 Rate constant dependence on light intensity

We began our analysis by comparing fluorescence rise curves in presence of DCMU at different light intensities. The purpose of such a procedure is to verify the photochemical character of the different phases. This also helped us to validate our method by comparing our results with those of Lazár et al. [27]. Due to the complexity and to the high number of parameters in equation 1, multiple possibilities exist for fitting the experimental data although they do not always have a biological sense. We thus force the fitting program to find common values for some parameters. In this case, connectivity and proportion of each type of photosystems had to remain unaltered between individuals sample. This makes sense since the only difference between samples is the intensity of illumination. Thus, the only parameter which may change are the rate constants of Q_A reduction k_i.

Figure 1A shows the DCMU-FR measured at different light intensities and the corresponding fits. The curves are plotted from time 0 to the time when rF_V reaches 1. Figure 1B shows the effect of light intensity on the rate constant values k for each type of photosystem. We see that for PSIIα and PSIIβ, the value is linearly correlated to the intensity of illumination, which confirms the photochemical character of the fluorescence rise for these two PSII types. This is not the case for PSIIγ (or γ phase) for which a different pattern is observed (Fi. 1B, inset). Therefore, the γ phase seems influenced by other factors than the absorption of light. This phase did not represente more than 4% of the variable fluorescence intensity (results not shown) while it represented a fraction of the CA that varied with light intensity. For this reason, determination of the kinetics and extent of this phase by the time course of the CA is considered not relevant. Thus in the subsequent analysis, phase γ was mathematically removed from the results to avoid any error in the determination of the proportion and kinetics of PSIIα and PSIIβ by the method of the CA.

Proportions, rate constants of photoreduction and connectivity of the three types of photosystem are detailed in table 2.

If one admits that the rate constant of a phase of the DCMU-FR curve reflects the size of the light-harvesting antenna associated with the corresponding type of PSII, it is possible to calculate the ratio $\frac{Chl_{PSII\alpha}}{Chl_{PSII\beta}}$ which is determined from the ratio of

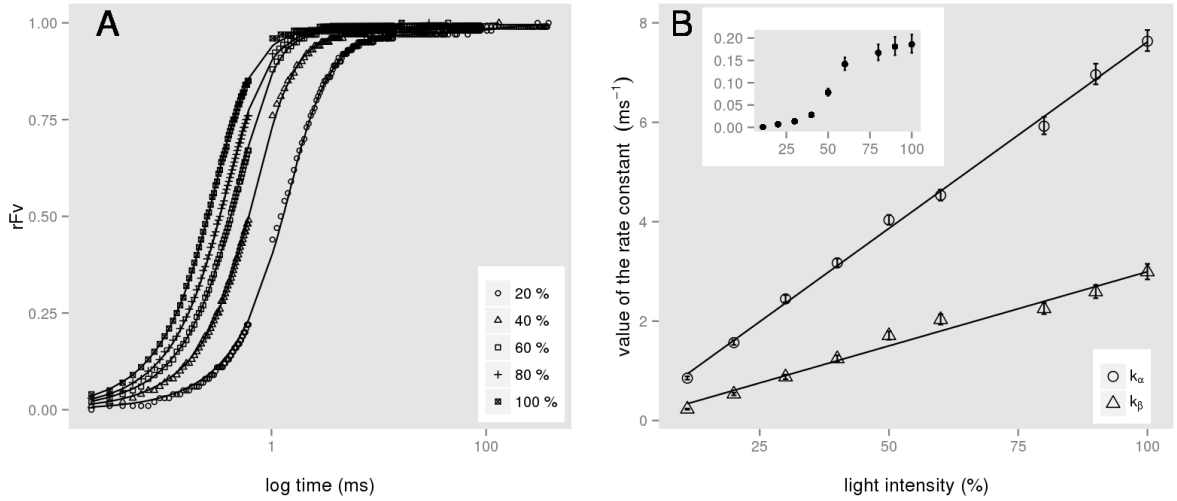

Figure 1: A: Time course of the DCMU-FR measured at different light intensities on the *wt* strain *1690* grown on Tris-buffered mineral media. Only 5 intensities are shown for clarity. 100 % = 1670 μmol PAR $m^{-2}s^{-1}$ PAR. Experimental curves and fits are shown as dots and full lines, respectively. B: value of the rate constant of photochemistry of PSIIα and PSIIβ plotted against the intensity of illumination. Inset shows the rate constant of photochemistry of PSIIγ. The errors bars were calculated according to section 2.5. Data are representative of one experiment out of at least three independent determinations.

type	%	k (s^{-1})	p
PSIIα	52	46.6 ± 1.4	0.75
PSIIβ	48	17.4 ± 2.4	0.58

Table 2: Proportion (%), rate constant of Q_A photoreduction (k) and connectivity (p) of each type of photosystem determined by fitting model 2 on FR-DCMU curves of the *wt* strain *1690* measured at different light intensities. Rate constant was determined by averaging individual rate constants for particular light intensities recalculated for an intensity of illumination of 10 μ mol PAR $m^{-2}s^{-1}$ in order to allow an easy comparison with previous studies (see Table 2 from Lazár et al. [27]).

$\frac{k_\alpha}{k_\beta}$ in most studies. However, the rate constant as determined in this study represents the kinetics of a whole phase and not the initial rate constant k_i^0 (see above). It is thus influenced not only by the antenna size but also by the connectivity. A better approach to calculate the ratio $\frac{Chl_{PSII\alpha}}{Chl_{PSII\beta}}$ is based on the proportion of each type of photosystems (ωPSII$_i$) and the proportion of chlorophyll fluorescence associated to them (FPSII$_i$) following equation 5 :

$$\frac{Chl_{PSII\alpha}}{Chl_{PSII\beta}} = \frac{F\text{PSII}_\alpha/\omega\text{PSII}_\alpha}{F\text{PSII}_\beta/\omega\text{PSII}_\beta} \quad (5)$$

The average ratio $\frac{Chl_{PSII\alpha}}{Chl_{PSII\beta}}$ determined here by this approach was 2.14 ± 0.39. This would mean that the PSIIα antenna is about 2-3 times larger than PSIIβ antenna if the pigments of both PSII types were equally excited. The excitation wavelength in this study (430 nm) however preferentially excites Chl a, which would tend to an overestimation of PSIIβ antenna size and proportion if the Chl $\frac{a}{b}$ is higher for PSIIβ. In earlier studies ratios between 1,65 and 8 were obtained (see Table 2 from Lazár et al. [27]). Such variations are probably caused by the different species and preparations studied.

The question arises whether the PSII heterogeneity evidenced here can be explained in terms of structural differences between the PSII populations that were previously separated using gel filtration [53, 54]. Only two functional populations of PSII are predicted by DCMU-FR analysis (PSIIα and PSIIβ) while gel filtration analysis predicts three different PSII populations (mega-, super- and core-complexes). Iwai, Takahashi, and Minagawa performed functional optical cross-section analysis on PSII fractions obtained by gel filtration separation [53]. Fractions composed mainly of PSII mega- and super- complexes had a similar optical cross section in contrast to the fraction composed mainly of PSII core complexes for which it was approximately two times lower. This indicates that PSII mega- and super- complexes are hardly distinguishable by functional analysis of the DCMU-FR since PSII an-

tenna size heterogeneity determination cannot discriminate two PSII populations with the same antenna size. It could be argued that although the antenna size of PSII mega- and super- complexes is the same, the connectivity may change. However, the accuracy for the decomposition of induction kinetics is not sufficient to reliably resolve them on this basis. Taking into account that the reduction rate constant found in this study for PSIIα is 2-3 times higher than for PSIIβ, it is tempting to conclude that PSIIα phase refers to PSII mega- and super- complexes and that PSIIβ phase refers to PSII core complexes.

3.2 The optical cross-section, as determined by the half-time of the fluorescence rise, is proportional to the proportion of PSIIα

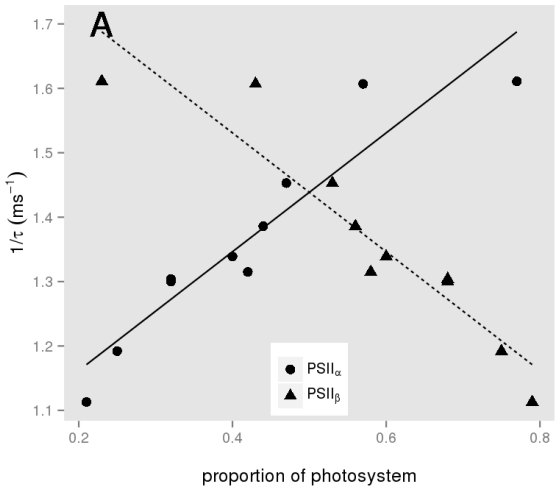

Figure 2: A: correlation between $\frac{1}{\tau}$ and the proportions of PSIIα and PSIIβ. τ is the time when the normalized variable fluorescence level reaches 0.5. R^2 for linear regression was 0.8 for both types of photosystem. The different *wt* strains (2',1690,25) were grown in different media (Tris-buffered acetate or mineral media).

To have an idea of the variations in the proportions of different PSII types in *Chlamydomonas reinhardtii*, we applied our analysis to several DCMU-FR of suspensions of different *wt* strains (2',1690,25) grown in different media (TAP, TMP, Bold) after dark-adaptation. We noticed large variations between samples. In other words, the proportions of PSIIα and PSIIβ vary extensively for dark-adapted cells.

We took advantage of these variations in order to investigate the relationship between the proportions of different PSII types and the half-time of the whole fluorescence rise, a parameter that is frequently used to characterize the PSII average optical cross-section e.g. [76, 77, 78, 79]. It is indeed possible to characterize the rate of the fluorescence rise by determining the half-time τ of the fluorescence increase as the time when the normalised variable fluorescence level reaches 0.5.

Figure 2B shows a positive and negative correlations between $\frac{1}{\tau}$ and the variable proportions of PSIIα and PSIIβ, respectively. In other words, the cell seems to adapt its ability to harvest light at PSII by converting fast PSIIα into slow PSIIβ and inversely. From these results, it appears that dark adaptation (usually used as standard condition) does not necessarily conduct to cells which are in the same state. It is known that growth condition can influence the amount of PSII-free and PSII-bound LHCII [80], thus modifying the ratio between different PSII types. This result could also explain the large variation in the determination of PSII heterogeneity observed in previous studies (see table 2 from Lazár et al. [27]) where amounts of PSIIα and PSIIβ ranged from 13.5% to 76% and from 9% to 40%, respectively.

type	k (s^{-1})	p
PSIIα	72.4 ± 9.9	0.89 ± 0.07
PSIIβ	14.1 ± 3.8	0.11 ± 0.21

Table 3: Summary of connectivity and rate constant of PSIIα and PSIIβ. Values are averages of the samples used in figure 2. Values of rate constant are recalculated for an intensity of illumination of 10 μ mol PAR $m^{-2}s^{-1}$ to allow an easy comparison with previous studies. Error ranges represent standard deviations.

Average values for rate constants of photoreduction (k) and connectivities (p) of PSIIα and PSIIβ are given in table 3. Values of k are in accordance with section 3.1 and previous studies (see Table 2 from Lazár et al. [27]). A non-zero connectivity term for PSIIβ is found again, although its value is here quite variable and lower compared to its value in section 3.1. The p value for PSIIα is higher than in section 3.1 and may be overestimated. Indeed, according to Lavergne and Trissl [72], it is possible to calculate the antenna size enhancement for open PSII surrounded by closed ones as J+1, where $J = p/(1-p)$, which makes J very sensitive to small errors in p determination. For a p value of 0.89, this antenna size enhancement would be around 9, which would indicate a connectivity between several super/mega complexes. Commonly

found p values around 0.7 give an antenna size enhancement of 3.3. Here, p values of 0,75 (section 3.1) and 0,62 (see below, section 3.4) lead to antenna size enhancements of 4.0 and 2.63, respectively, which do not require connectivity between super/mega complexes. More data and higher reliability on p would be necessary to conclude on this issue.

The variations in PSII heterogeneity and in half-time of the fluorescence rise from one sample to another were most probably due to uncontrolled variations in the PQ pool redox state. Such variations are easily produced as consequences of changes in the medium composition of cultured cells (acetate concentration), or depending on the extent of aeration of the culture and dark-adaptation time before measurements. Therefore, changes in PSII optical cross-section from one sample to another were most probably due to changes in metabolic status of the cells and thus to changes in excitation energy distribution between PSII and PSI (state transitions). In the next sections, we investigated changes in PSII heterogeneity during experimentally controlled state transitions.

3.3 Development of a protocol to determine PSII antenna size heterogeneity during state transition

We then tried to determine the changes in PSII antenna size heterogeneity during state transitions. To trigger a transition from state 1 to state 2, we used the method described by Bulté et al. [81], which consists of inhibiting mitochondrial respiration either by using inhibitors/uncouplers of respiration, or by anoxia. Impairment of mitochondrial respiration leads to a depletion of ATP and a non-photochemical reduction of the PQ pool by the NAD(P)H dehydrogenase NDA2, thus inducing a transition to state 2. State 1 (or a state close to it) is usually achieved first by dark-adapting well-aerated cells in order to oxidize the PQ pool (this is only valid for cells grown on mineral media).

To determine PSII heterogeneity, we performed measurements of the DCMU-FR on cells dark-adapted for 30 min (state 1) or cells in presence of mitochondrial inhibitors KCN (potassium cyanide) and SHAM (salicylhydroxamic acid) for 20 min (state 2). The fluorescence rise was first found faster in state 2 than in state 1 which is in contradiction with the common sense if PSII antenna size is smaller in state 2. The results were similar if mitochondrial respiration was impaired by the addition of the uncoupler FCCP or by an anoxia caused by the addition of glucose oxydase and glucose (results not shown). In state 2 condition, there was an increase and a decrease in F_O and F_M levels, respectively. The decrease of F_M is explained by the reduced PSII antenna size in state 2. The increase of F_O can be explained by the fact that binding of DCMU in the dark can induce a back transfer of electron from PSII-bound semiquinone Q_B^- to Q_A [82, 83]. In the case when the PQ pool is highly reduced like in state 2 inducing conditions (due to a constant non-photochemical reduction) many PSII centers may have a Q_B^- bound and the addition of DCMU leads to Q_A reduction before the illumination. Therefore, in this situation, the fluorescence rise under illumination only represents a small pool of initially oxidized PSII.

In order to probe all the PSII pool in state 2, PQ pool had to be rapidly oxidized before the addition of DCMU. We thus used a different approach to reoxidize the PQ pool after reaching state 2. For this, instead of using respiration inhibitors to induce PQ reduction and state 2, we bubbled N_2 in a closed electrode chamber of algal suspension and let the cells consume the remaining O_2 through respiration in order to cause anoxia and a transition to state 2. When state 2 was reached, opening of the electrode chamber and adding air led to the arrest of non-photochemical reduction and to re-oxidation of the PQ pool. This was confirmed by PAM fluorimetry measurements during the whole procedure (Fig. 3). The fluorescence level of PSII measured under low analytic modulated light is dependent on the redox state of Q_A in the reaction center of PSII and, indirectly, by the subsequent intermediates in the photosynthetic electron transport chain together with state transitions. In order to monitor the redox state of Q_A without the influence of state transitions, we first performed experiments with the mutant strain *stt7* which lacks the ability to realize state transition. Figure 3A shows the PAM fluorescence trace of the *stt7* strain. Removal of oxygen induces a rapid increase of F_O which reflects the non-photochemical reduction of PQ pool. Then, addition of oxygen (air) induces a fast decrease of F_O which reflects the re-oxidation of PQ pool, thus confirming that PQ pool can be oxidized almost instantly by O_2 most probably via the plastid terminal oxydaze (PTOX).

In contrast to the *stt7* strain, the increase of F_O after removal of oxygen in the *wt* strain *1690* (Fig 3B) is not so apparent because it is counterbalanced by a general fluorescence decrease due to detachment of LHCII from PSII (transition to state 2) as indicated by the decrease of maximum level F'_M. Addition of oxygen after transition to state 2 leads to a slight decrease of F_O which reflects PQ pool

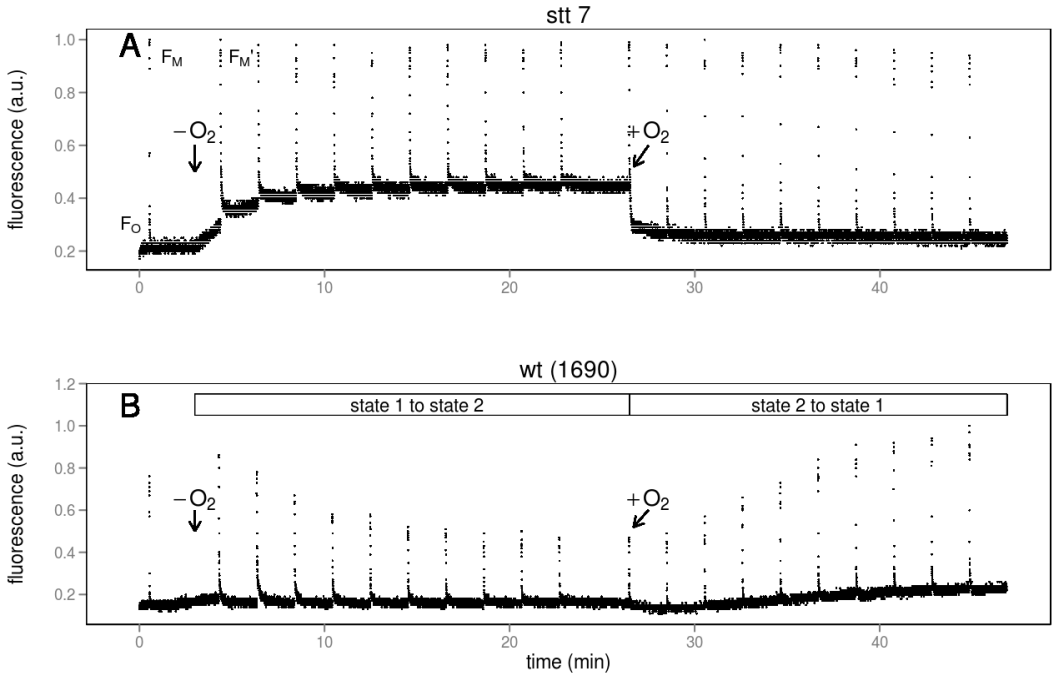

Figure 3: Determination of changes in the redox status of PQ pool and state transitions by PAM fluorimetry as described in section 2.3. A: state transition deficient mutant *stt7*. B: wild type strain *1690*. Strains were grown on Tris-buffered acetate media. O_2 is removed or added when indicated. Removal is realized by bubbling N_2 and closing the electrode chamber and addition is realized by opening the closed chamber and bubbling air. Data are representative of one experiment out of at least three independent determinations.

re-oxidation. This is followed by a transition back to state 1 as indicated by the increase of $F_M^{'}$ caused by the re-association of LHCII to PSII.

In both cases (*stt7* and *wt* strains), the re-oxidation of PQ pool by O_2 is realized in less than 2 minutes after its addition (as indicated by the duration of the decrease of F_O). Moreover, in the *wt* strain, F_M did not increase within this time, indicating that back transition to state 1 did not start yet (this is confirmed by the non-significant variation in the low temperature fluorescence ratio between 0 and 2 min after O_2 addition, see fig 4A). Therefore, PSII antenna heterogeneity analysis could be realized on samples taken from 2 min after the addition of O_2 (state 2) to the end of the transition to state 1.

3.4 Transition to state 2 from state 1 is reflected in conversion of PSIIα and PSIIβ

PSII antenna heterogeneity variations were determined on samples taken from 2 to 20 minutes after addition of O_2. First, it was verified that state transition was occurring in theses samples by measuring low temperature (77K) fluorescence spectra. At this temperature, fluorescence emission by PSI and PS II can be distinguished. The 685 nm fluorescence is emitted by PSII while the 715 nm fluorescence is emitted by PSI. Variation of this ratio indicates variation in distribution of excitation energy between PSI and PSII. Figure 4A shows a decrease of the ratio F715/(715+685) from 2 minutes to 20 minutes after O_2 addition in the case of *wt*

	p_α	p_β	k_α (s^{-1})	k_β (s^{-1})	$\frac{k_\alpha}{k_\beta}$
wt	0.62	0.15	48.6	15.4	3.1
stt7	0.64	0.16	64	19	3.3

Table 4: Summary of connectivity and rate constant of PSIIα and PSIIβ. Values are averages of the 7 samples used in figure 4. Values of rate constant are recalculated for an intensity of illumination of 10 μ mol PAR $m^{-2}s^{-1}$ to allow an easy comparison with previous studies. Data are representative of one experiment out of at least three independent determinations.

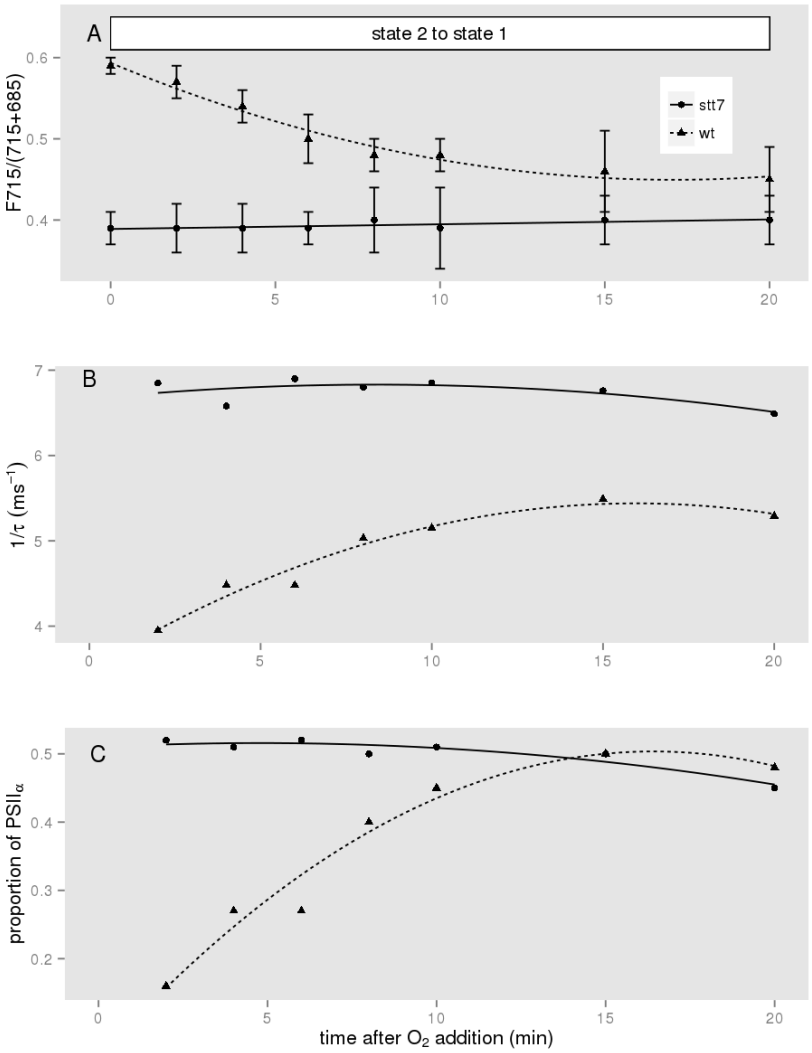

Figure 4: A: variation in the ratio of fluorescence emitted at 715 and 685 nm at 77 K indicating a state transition from state 2 to state 1 in the *wt* strain but not in the *stt7* strain. Each value is the mean of 3 independent experiments. Error bars represent standard deviations. B: variation of $\frac{1}{\tau}$ indicating a decrease of the optical cross-section of PSII during transition from state 2 to state 1. C: Variations in proportions of PSIIα during transition from state 2 to state 1. DCMU-FR were measured at 100% of maximal light intensity. Strains were grown on Tris-buffered acetate media. For B and C, data are representative of one experiment out of at least three independent determinations.

strain, indicating a transition from state 2 to state 1 (high and low values of F715/(715+685), respectively). In contrast, in the *stt7* strain, there is no significant variation of this ratio, as expected.

We then determined changes in proportions and properties of PSIIα and PSIIβ from DCMU-FR curves during the transition from state 2 to state 1. Since biochemical studies on PSII complexes indicate that state transitions are caused by changes in relative abundances in different PSII subpopulations [53, 54], we forced the fitting program to find common values for rate constants of photoreduction (k) and connectivity (p) for each PSII type during state transition. Fits and corresponding residuals for the *wt* strain 1690 in state 1 and in state 2 (corresponding to 2 and 20 min after O_2 addition, respectively) are shown in figure S2. Rate constants of photoreduction (k) and connectivities (p) of PSIIα and PSIIβ for the *wt* and *stt7* strains are detailed in table 4. Values of k and p are in accordance with previous section and previous studies (see Table 2 from Lazár et al. [27]).

Changes in proportions of PSIIα in the course of state transition are shown in figure 4C. In the *wt* strain, during transition from state 2 to state 1, about 32% of slow PSIIβ is converted into fast PSIIα with the same kinetics than the variation of the ratio F715/(715+685) and the half-time of the whole fluorescence rise. In contrast, no significant variation is observed in the state transition deficient strain *stt7*. These results show for the first time *in vivo* that state transition induces an interconversion of two types of photosystems.

This is in agreement with recent models based on biochemical and structural analysis of PSII after gel filtration separation which indicate a conversion of PSII mega- and super- complexes (that we suggest to be related to PSIIα) in PSII core complexes (that we suggest to be related to PSIIβ) during state transitions [53, 54]. In contrast to the frequent implicit view that state 1 and state 2 are characterized by specific PSII states, it appears that the two PSII populations are present in both states but in different proportions.

4 Conclusion

In this study, we showed that variations in the optical cross-section of PSII (as indicated by half-time estimations of the DCMU-FR) can be described as changes in PSIIα/PSIIβ heterogeneity. Our results on PSII heterogeneity during a transition from state 2 to state 1 showed for the first time *in vivo* that this transition correlates with a conversion of PSIIβ to PSIIα. Considering our results and recent biochemical and structural researches on PSII, we suggest that in *Chlamydomonas reinhardtii* PSIIα refers to two PSII populations with the same antenna size and a high degree of connectivity, namely the PSII mega- and super- complexes whereas PSIIβ refers to a PSII population with a 2-3 times smaller antenna size and a reduced connectivity, namely the PSII core complexes. We think that the procedure of PSII antenna size heterogeneity determination described in this study could be useful to study PSII antenna size heterogeneity in other photosynthetic organisms as well as in antenna size mutants.

5 Acknowledgments

This study was supported by FP7-funded Sunbiopath project (GA 245070). Thomas de Marchin thanks the F.R.I.A. for the award of a fellowship. Fabrice Franck is senior research associate of the Fonds de la Recherche Scientifique F.R.S-FNRS. Many thanks are given to Dr F.A. Wollman, Dr P. Tocquin and Dr P. Cardol and the anonymous reviewers for their helpful suggestions during this work.

References

[1] C. Bonaventura and J. Myers. “Fluorescence and oxygen evolution from Chlorella pyrenoidosa”. In: *BBA-Bioenergetics* 189.3 (1969), pp. 366–383.

[2] N. Murata. “Control of excitation transfer in photosynthesis I. Light-induced change of chlorophyll a fluoresence in Porphyridium cruentum”. In: *BBA-Bioenergetics* 172.2 (1969), pp. 242–251.

[3] R. Delosme, J. Olive, and F. A. Wollman. “Changes in light energy distribution upon state transitions: an in vivo photoacoustic study of the wild type and photosynthesis mutants from Chlamydomonas reinhardtii”. In: *BBA-Bioenergetics* 1273.2 (1996), 150–158.

[4] A. V. Vener et al. “Plastoquinol at the quinol oxidation site of reduced cytochrome bf mediates signal transduction between light and protein phosphorylation: thylakoid protein kinase deactivation by a single-turnover flash”. In: *PNAS* 94.4 (1997), 1585–1590.

[5] F. Zito et al. “The Qo site of cytochrome b6f complexes controls the activation of the LHCII kinase”. In: *EMBO J.* 18.11 (1999), 2961–2969.

[6] N. Depege, S. Bellafiore, and J. Rochaix. “Role of Chloroplast Protein Kinase Stt7 in LHCII Phosphorylation and State Transition in Chlamydomonas”. In: *Science* 299.5612 (2003), pp. 1572–1575.

[7] A. Shapiguzov et al. “The PPH1 phosphatase is specifically involved in LHCII dephosphorylation and state transitions in Arabidopsis”. In: *PNAS* 107.10 (2010), pp. 4782–4787.

[8] M. Pribil et al. “Role of Plastid Protein Phosphatase TAP38 in LHCII Dephosphorylation and Thylakoid Electron Flow”. In: *PLoS Biol.* 8.1 (2010). Ed. by J. Chory, e1000288.

[9] E. Rintamäki et al. “Cooperative regulation of light-harvesting complex II phosphorylation via the plastoquinol and ferredoxin-thioredoxin system in chloroplasts”. In: *PNAS* 97.21 (2000), p. 11644.

[10] G. Finazzi et al. “State transitions, cyclic and linear electron transport and photophosphorylation in Chlamydomonas reinhardtii”. In: *BBA-Bioenergetics* 1413.3 (1999), 117–129.

[11] F. A Wollman. “State transitions reveal the dynamics and flexibility of the photosynthetic apparatus”. In: *EMBO J.* 20.14 (2001), 3623–3630.

[12] D. I. Arnon, H. Y. Tsujimoto, and B. D. Mcswain. “Ferredoxin and Photosynthetic Phosphorylation”. In: *Nature* 214.5088 (1967), pp. 562–566.

[13] D. I. Arnon and R. K. Chain. “Regulation of ferredoxin-catalyzed photosynthetic phosphorylations”. In: *PNAS* 72.12 (1975), pp. 4961–4965.

[14] P. Joliot and A. Joliot. “Cyclic electron transfer in plant leaf”. In: *PNAS* 99.15 (2002), pp. 10209–10214.

[15] J. M. Anderson and A. Melis. “Localization of different photosystems in separate regions of chloroplast membranes”. In: *PNAS* 80.3 (1983), p. 745.

[16] O Vallon, F. Wollman, and J Olive. “Lateral distribution of the main protein complexes of the photosynthetic apparatus in Chlamydomonas reinhardtii and in spinach: an immunocytochemical study using intact thylakoid membranes and a PSII enriched membrane preparation”. In: *Photobiochem. Photobiophys* 12 (1986), pp. 203–220.

[17] P Joliot and A Joliot. “Etude cinétique de la réaction photochimique libérant de l’oxygène au cours de la photosynthèse”. In: *CR Acad. Sci. Paris* 258 (1964), pp. 4622–4625.

[18] W. W. Doschek and B. Kok. “Photon Trapping in Photosystem II of Photosynthesis: The Fluorescence Rise Curve in the Presence of 3-(3,4-Dichlorophenyl)-1,1-dimethylurea”. In: *Biophys. J.* 12.7 (1972), pp. 832–838.

[19] A. Melis and P. H. Homann. “Kinetic analysis of the fluorescence induction in 3-(3,4-dichlorophenyl)-1,1-dimethylurea poisoned chloroplasts”. In: *Photochem. Photobiol.* 21.6 (1975), pp. 431–437.

[20] A Melis and P. H. Homann. “Heterogeneity of the photochemical centers in system II of chloroplasts”. In: *Photochem. Photobiol.* 23.5 (1976), pp. 343–350.

[21] N. Murata, M. Nishimura, and A. Takamiya. “Fluorescence of chlorophyll in photosynthetic systems II. Induction of fluorescence in isolated spinach chloroplasts”. In: *BBA - Biophys. incl. Photos.* 120.1 (1966), pp. 23–33.

[22] P. Bennoun and Y.-s. Li. “New results on the mode of action of 3,-(3,4-dichlorophenyl)-1,1-dimethylurea in spinach chloroplasts”. In: *BBA-Bioenergetics* 292.1 (1973), pp. 162–168.

[23] S. Malkin and B. Kok. “Fluorescence induction studies in isolated chloroplasts. I. Number of components involved in the reaction and quantum yields.” In: *BBA* 126.3 (1966), p. 413.

[24] B. Hsu and J. Lee. “A study on the fluorescence induction curve of the DCMU-poisoned chloroplast”. In: *BBA-Bioenergetics* 1056.3 (1991), pp. 285–292.

[25] B. Hsu, Y. Lee, and Y. Jang. “A method for analysis of fluorescence induction curve from DCMU-poisoned chloroplasts”. In: *BBA-Bioenergetics* 975.1 (1989), pp. 44–49.

[26] A. Melis and J. M. Anderson. “Structural and functional organization of the photosystems in spinach chloroplasts. Antenna size, relative electron-transport capacity, and chlorophyll composition”. In: *BBA-Bioenergetics* 724.3 (1983), pp. 473–484.

[27] D. Lazár et al. “Determination of the antenna heterogeneity of Photosystem II by direct simultaneous fitting of several fluorescence rise curves measured with DCMU at different light intensities”. In: *Photosynth. Res.* 68.3 (2001), 247–257.

[28] J. Sinclair and S. M. Spence. “Heterogeneous photosystem 2 activity in isolated spinach chloroplasts”. In: *Photosynth. Res.* 24.3 (1990), 209–220.

[29] J. Lavergne and J.-M. Briantais. “Photosystem II heterogeneity”. In: *Oxygenic photosynthesis: The light reactions*. Springer, 2004, pp. 265–287.

[30] L. Duysens and H. Sweers. “Mechanism of two photochemical reactions in algae as studied by means of fluorescence”. In: *Studies on microalgae and photosynthetic bacteria* (1963), pp. 353–372.

[31] A. Stirbet et al. “Chlorophyll a fluorescence induction: a personal perspective of the thermal phase, the J–I–P rise”. In: *Photosynth. Res.* 113.1-3 (2012), pp. 15–61.

[32] N. Moise and I. Moya. “Correlation between lifetime heterogeneity and kinetics heterogeneity during chlorophyll fluorescence induction in leaves:: 1. Mono-frequency phase and modulation analysis reveals a conformational change of a PSII pigment complex during the IP thermal phase”. In: *BBA-Bioenergetics* 1657.1 (2004), pp. 33–46.

[33] N. Moise and I. Moya. “Correlation between lifetime heterogeneity and kinetics heterogeneity during chlorophyll fluorescence induction in leaves: 2. Multi-frequency phase and modulation analysis evidences a loosely connected PSII pigment–protein complex”. In: *BBA-Bioenergetics* 1657.1 (2004), pp. 47–60.

[34] G. Schansker et al. “Evidence for a fluorescence yield change driven by a light-induced conformational change within photosystem II during the fast chlorophyll a fluorescence rise”. In: *BBA-Bioenergetics* 1807.9 (2011), pp. 1032–1043.

[35] A. Melis and L. N. M. Duysens. “Biphasic Energy Conversion Kinetics and Absorbance Difference Spectra of Photosystem II of Chloroplasts. Evidence for Two Different Photosystem II Reaction Centers”. en. In: *Photochem. Photobiol.* 29.2 (1979), 373–382.

[36] J. Lavergne and F. Rappaport. “Stabilization of charge separation and photochemical misses in photosystem II”. In: *Biochemistry-US* 37.21 (1998), 7899–7906.

[37] P. Joliot and A. Joliot. “Evidence for a double hit process in Photosystem II based on fluorescence studies”. In: *BBA-Bioenergetics* 462.3 (1977), pp. 559–574.

[38] A. Thielen and H. van Gorkom. “Quantum efficiency and antenna size of Photosystems IIα, IIβ and I in tobacco chloroplasts”. In: *BBA-Bioenergetics* 635.1 (1981), pp. 111–120.

[39] T. A. Roelofs, C.-H. Lee, and A. R. Holzwarth. “Global target analysis of picosecond chlorophyll fluorescence kinetics from pea chloroplasts: A new approach to the characterization of the primary processes in photosystem II α- and β-units”. In: *Biophys. J.* 61.5 (1992), pp. 1147–1163.

[40] U. Schreiber and K. Pfister. “Kinetic analysis of the light-induced chlorophyll fluorescence rise curve in the presence of dichlorophenyldimethylurea: Dependence of the slow-rise component on the degree of chloroplast intactness”. In: *BBA-Bioenergetics* 680.1 (1982), pp. 60–68.

[41] M. T Black, T. H Brearley, and P. Horton. “Heterogeneity in chloroplast photosystem II”. In: *Photosynth. Res.* 8.3 (1986), 193–207.

[42] D. J. Kyle, P. Haworth, and C. J. Arntzen. “Thylakoid membrane protein phosphorylation leads to a decrease in connectivity between photosystem II reaction centers”. In: *BBA-Bioenergetics* 680.3 (1982), 336–342.

[43] P. Horton and M. T. Black. “Light-dependent quenching of chlorophyll fluorescence in pea chloroplasts induced by adenosine 5’-triphosphate”. In: *BBA-Bioenergetics* 635.1 (1981), pp. 53–62.

[44] P. Horton and M. T. Black. “A comparison between cation and protein phosphorylation effects on the fluorescence induction curve in chloroplasts treated with 3-(3,4-dichlorophenyl)-1,1-dimethylurea”. In: *BBA-Bioenergetics* 722.1 (1983), pp. 214–218.

[45] L. Nedbal, M. Trtílek, and D. Kaftan. “Flash fluorescence induction: a novel method to study regulation of Photosystem II”. In: *J. Photochem. Photobiol. B* 48.2-3 (1999), pp. 154–157.

[46] S. Mathur, S. Allakhverdiev, and A. Jajoo. “Analysis of high temperature stress on the dynamics of antenna size and reducing side heterogeneity of Photosystem II in wheat leaves Triticum aestivum”. In: *BBA-Bioenergetics* 1807.1 (2011), 22–29.

[47] N. G. Bukhov and R. Carpentier. “Heterogeneity of photosystem II reaction centers as influenced by heat treatment of barley leaves”. In: *Physiol. Plant.* 110.2 (2000), 279–285.

[48] A. Melis and G. Akoyunoglou. “Development of the two heterogeneous Photosystem II units in etiolated bean leaves”. In: *Plant Physiol.* 59.6 (1977), p. 1156.

[49] X. Barthélemy, R. Popovic, and F. Franck. “Studies on the O-J-I-P transient of chlorophyll fluorescence in relation to photosystem II assembly and heterogeneity in plastids of greening barley”. In: *J. Photochem. Photobiol. B* 39.3 (1997), pp. 213–218.

[50] E. J. Boekema et al. “Arrangement of photosystem II supercomplexes in crystalline macrodomains within the thylakoid membrane of green plant chloroplasts”. In: *J. Mol. Biol.* 301.5 (2000), pp. 1123–1133.

[51] R. Kouřil, J. P. Dekker, and E. J. Boekema. "Supramolecular organization of photosystem II in green plants". In: *Biochimica et Biophysica Acta (BBA)-Bioenergetics* 1817.1 (2012), pp. 2–12.

[52] J. Nield, K. Redding, and M. Hippler. "Remodeling of light-harvesting protein complexes in Chlamydomonas in response to environmental changes". In: *Eukaryot. Cell* 3.6 (2004), 1370–1380.

[53] M. Iwai, Y. Takahashi, and J. Minagawa. "Molecular remodeling of photosystem II during state transitions in Chlamydomonas reinhardtii". In: *Plant Cell* 20.8 (2008), p. 2177.

[54] J. Minagawa. "State Transitions–the molecular remodeling of photosynthetic supercomplexes that controls energy flow in the chloroplast". In: *BBA-Bioenergetics* 1807.8 (2011), pp. 897–905.

[55] D. Kyle, L. Staehelin, and C. Arntzen. "Lateral mobility of the light-harvesting complex in chloroplast membranes controls excitation energy distribution in higher plants". In: *Arch. Biochem. Biophys.* 222.2 (1983), pp. 527–541.

[56] M. T. Black, P. Lee, and P. Horton. "Changes in topography and function of thylakoid membranes following membrane protein phosphorylation". In: *Planta* 168.3 (1986), 330–336.

[57] U. K. Larsson, B. Jergil, and B. Andersson. "Changes in the lateral distribution of the light-harvesting chlorophyll-a/b—protein complex induced by its phosphorylation". In: *Eur. J. Biochem.* 136.1 (1983), 25–29.

[58] H. Takahashi et al. "Identification of the mobile light-harvesting complex II polypeptides for state transitions in Chlamydomonas reinhardtii". In: *PNAS* 103.2 (2006), pp. 477–482.

[59] A. V. Ruban and M. P. Johnson. "Dynamics of higher plant photosystem cross-section associated with state transitions". In: *Photosynth. Res.* 99 (2008), pp. 173–183.

[60] R. Tokutsu, M. Iwai, and J. Minagawa. "CP29, a Monomeric Light-harvesting Complex II Protein, Is Essential for State Transitions in Chlamydomonas reinhardtii". In: *J. Biol. Chem.* 284.12 (2009), pp. 7777–7782.

[61] J. García-Cerdán et al. "The PsbW protein stabilizes the supramolecular organization of photosystem II in higher plants". In: *Plant J.* 65.3 (2011), pp. 368–381.

[62] L. Dietzel et al. "Photosystem II Supercomplex Remodeling Serves as an Entry Mechanism for State Transitions in Arabidopsis". In: *Plant Cell* 23.8 (2011), pp. 2964–2977.

[63] M. M. Fleischmann et al. "Isolation and Characterization of Photoautotrophic Mutants of Chlamydomonas reinhardtii Deficient in State Transition". In: *J. Biol. Chem.* 274.43 (1999), 30987–30994.

[64] D. S Gorman and R. P. Levine. "Cytochrome f and plastocyanin: their sequence in the photosynthetic electron transport chain". In: *PNAS* 54.6 (1965), p. 1665.

[65] D. R. Davies and A. Plaskitt. "Genetical and Structural Analyses of Cell-Wall Formation in Chlamydomonas Reinhardi". In: *Genet. Res.* 17.01 (1971), pp. 33–43.

[66] E. H. Harris. *The Chlamydomonas Sourcebook: A Comprehensive Guide to Biology and Laboratory Use*. Academic Press Inc, 1989.

[67] Lichtenthaler. "Chlorophylls and carotenoids: pigment of photosynthetic biomembranes." In: *Methods Enzymol.* 148.148 (1987), pp. 350–382.

[68] R. D. C. Team. *R: A Language and Environment for Statistical Computing*. ISBN 3-900051-07-0. Vienna, Austria, 2011.

[69] J. Pinheiro et al. *nlme: Linear and Nonlinear Mixed Effects Models*. R package version 3.1-102. 2011.

[70] M. L. Johnson, L. M. Faunt, et al. "Parameter estimation by least-squares methods". In: *Methods Enzymol.* 210.1 (1992), p. 37.

[71] D. H. Bell and M. F. Hipkins. "Analysis of fluorescence induction curves from pea chloroplasts: Photosystem II reaction centre heterogeneity". In: *BBA-Bioenergetics* 807.3 (1985), pp. 255–262.

[72] J. Lavergne and H. Trissl. "Theory of fluorescence induction in photosystem II: derivation of analytical expressions in a model including exciton-radical-pair equilibrium and restricted energy transfer between photosynthetic units". In: *Biophys. J.* 68.6 (1995), pp. 2474–2492.

[73] H. Trissl and J. Lavergne. "Fluorescence induction from photosystem II: analytical equations for the yields of photochemistry and fluorescence derived from analysis of a model including exciton-radical pair equilibrium and restricted energy transfer between photosynthetic units". In: *Aust. J. Plant Physiol.* 22.2 (1995), 183–193.

[74] H. Akaike. “A new look at the statistical model identification”. In: *IEEE Trans. Autom. Control* 19.6 (1974), pp. 716–723.

[75] K. P. Burnham and D. R. Anderson. *Model Selection and Multimodel Inference: A Practical Information-theoretic Approach*. Springer, 2002.

[76] J. Lavaud et al. “Influence of the diadinoxanthin pool size on photoprotection in the marine planktonic diatom Phaeodactylum tricornutum”. In: *Plant Physiol.* 129.3 (2002), 1398–1406.

[77] M. Havaux and F. Tardy. “Loss of chlorophyll with limited reduction of photosynthesis as an adaptive response of Syrian barley landraces to high-light and heat stress”. In: *Aust. J. Plant Physiol.* 26.6 (1999), 569–578.

[78] J.-C. Cadoret et al. “Dissipation of excess energy triggered by blue light in cyanobacteria with CP43 (isiA)”. In: *BBA-Bioenergetics* 1659.1 (2004), pp. 100–104.

[79] L. Dall’Osto et al. “Lutein is needed for efficient chlorophyll triplet quenching in the major LHCII antenna complex of higher plants and effective photoprotection in vivo under strong light”. In: *BMC Plant. Biol.* 6.1 (2006), p. 32.

[80] J. M. Anderson. “Photoregulation of the composition, function, and structure of thylakoid membranes”. In: *Annu. Rev. Plant. Physiol.* 37.1 (1986), 93–136.

[81] L. Bulté et al. “ATP control on state transitions in vivo in Chlamydomonas reinhardtii”. In: *BBA-Bioenergetics* 1020.1 (1990), pp. 72–80.

[82] B. Velthuys and J Amesz. “Charge accumulation at the reducing side of system 2 of photosynthesis”. In: *BBA-Bioenergetics* 333.1 (1974), pp. 85–94.

[83] L. Bulté and F. Wollman. “Stabilization of states I and II by p-benzoquinone treatment of intact cells of Chlamydomonas reinhardtii”. In: *BBA-Bioenergetics* 1016.2 (1990), pp. 253–258.

Supplemental data

There is no explicit solution to the equations (1), (2) and (3)

By re-writing equation (1), one can explicitly express PSII_i^{closed} as a function of $rF_{V,i}$ and p_i :

$$\mathrm{PSII}_i^{closed}(t) = \frac{rF_{V,i}(t)}{p_i rF_{V,i}(t) + 1 - p_i}. \quad (6)$$

Combined with equation (2), this equation leads to

$$e^{-k_i(t)t} = \frac{\big(1 - rF_{V,i}(t)\big)(1 - p_i)}{1 - p_i(1 - rF_{V,i}(t))}. \quad (7)$$

One thus have,

$$k_i(t) = \frac{1}{t}\Big(\ln\Big(1 - p_i\big(1 - rF_{V,i}(t)\big)\Big) - \ln\big(1 - rF_{V,i}(t)\big) - \ln(1 - p_i)\Big). \quad (8)$$

Finally, equation (3) implies

$$\mathrm{k}_i^0 = \frac{1 - p_i}{t\big(p_i rF_{V,i}(t) + 1 - p_i\big)} \Big(\ln\big(1 - p_i(1 - rF_{V,i}(t))\big) - \ln\big(1 - rF_{V,i}(t)\big) - \ln(1 - p_i)\Big). \quad (9)$$

This relation shows that k_i^0 depends on p_i and $rF_{V,i}$, both being unknown. Therefore k_i^0 cannot be determined using a non-linear regression algorithm simultaneously with other parameters of equations (1) and (2).

Residuals of the fit for model 1, 2 and 3

Figure S1 indicates that model 1 is worse than model 2 and model 3 in describing the experimental data. The residuals of model 2 and model 3 are identical because a 0 connectivity is found for γ phase in model 3. Thus, the fit is exactly the same for model 2 and model 3. The choice of model 2 by the AIC criterion is based on the reduced number of parameters in this model.

Fits and corresponding residuals for state 1 and for state 2

Upper panel of figure S2 shows a decrease in the rate of fluorescence increase under illumination in state 2 compared to state 1, as expected. Lower panel shows that the residuals for the fit in state 1 and in state 2 are small. This indicates that the fit prediction is very close to the experimental data.

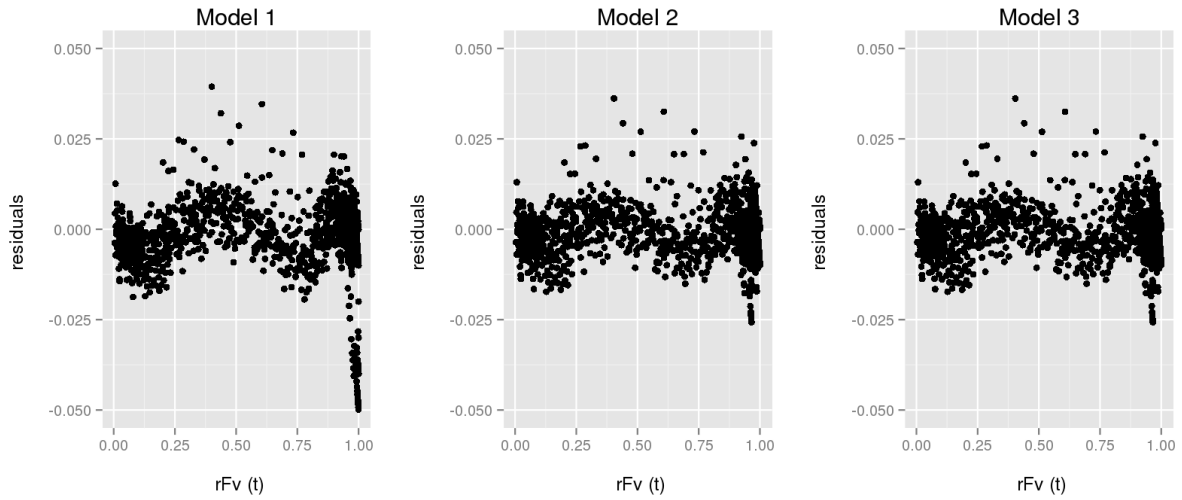

Figure S1: Residuals of the fits on data of section 3.1 for model 1 (connectivity allowed only for PSIIα) , model 2 (connectivity allowed for PSIIα and PSIIβ) and model 3 (connectivity allowed for PSIIα, PSIIβ and PSIIγ).

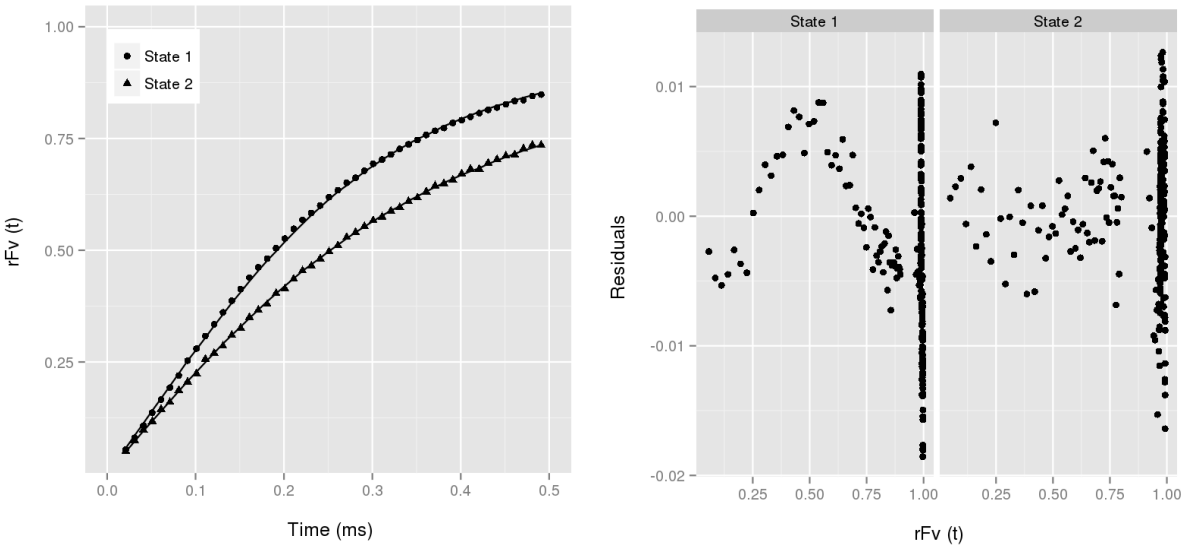

Figure S2: Upper panel, DCMU-FR of *wt* strain 1690 in state 1 and in state 2. Symbols : experimental data, line : fit. Lower panel, Residuals for the fits in state 1 and in state 2.